Radiation Measurements 55 (2013) 128–131

Contents lists available at SciVerse ScienceDirect

Radiation Measurements

journal homepage: www.elsevier.com/locate/radmeas

Neutron detection with $LiCaAlF_6$ scintillator doped with 3d-transition metal ions

Noriaki Kawaguchi [a,b,c,*], Takayuki Yanagida [d], Yutaka Fujimoto [b], Yuki Furuya [b], Yoshisuke Futami [b], Akihiro Yamaji [b], Kenichi Watanabe [e], Atsushi Yamazaki [e], Akira Uritani [e], Shinji Kajimoto [c], Hiroshi Fukumura [c], Shunsuke Kurosawa [b], Yuui Yokota [b], Jan Pejchal [b], Akira Yoshikawa [b]

[a] Tokuyama Corporation, Shibuya 3-chome, Shibuya-ku, Tokyo 150-8383, Japan
[b] IMR, Tohoku University, 2-1-1 Katahira, Aoba-ku, Sendai, Miyagi 980-8577, Japan
[c] Department of Chemistry, Graduate School of Science, Tohoku University, 6-3 Aoba, Aramaki, Aoba-ku, Sendai, Miyagi 980-8578, Japan
[d] Kyushu Institute of Technology, 2-4 Hibikino, Wakamatsu-ku, Kitakyushu, Fukuoka 808-0135, Japan
[e] Department of Quantum Engineering, Nagoya Univ., Furo-cho, Chikusa-ku, Nagoya 464-8603, Japan

HIGHLIGHTS

- Neutron detection with 3d-transition metal ions doped $LiCaAlF_6$ is investigated.
- Single crystals of Ti, V, Mn, Fe, Co, Ni and Cu doped $LiCaAlF_6$ are grown.
- In α-ray induced emission spectra, Mn doped $LiCaAlF_6$ showed highest intensity.
- Mn doped $LiCaAlF_6$ coupled with Si-APD exhibited a clear neutron signal.

ARTICLE INFO

Article history:
Received 31 March 2012
Received in revised form
13 March 2013
Accepted 16 March 2013

Keywords:
Scintillator
Neutron
Single crystal
Fluoride

ABSTRACT

Capability of thermal neutron detection was examined for $LiCaAlF_6$ (LiCAF) scintillators doped with 3d-transition metal ions. Their radioluminescence spectra were measured with an 241-Am source to simulate $^6Li(n, \alpha)^3H$ reaction. The sufficiently intense radioluminescence was observed for the Mn, Co and Cu dopants, while only a weak one was observed for Ti, V, Fe and Ni. A Mn doped LiCAF crystal, which showed the highest radioluminescence intensity, was coupled with a Si avalanche photodiode for the examination of its neutron response. It was confirmed that the average current of the photodiode clearly increased under excitation with 13.5 meV neutron flux.

1. Introduction

Scintillators are widely used in many applications of ionizing radiation, such as medical imaging or therapy (Yanagida et al., 2010), well-logging (Nikitin and Bliven, 2010), and basic physics research (Yamaoka et al., 2005). Some of these applications are the monitoring and imaging applications. The development of imaging and monitoring techniques using neutrons has started in the recent past. ^3He gas used in gas counters proved to be suitable and efficient solution. However, the contemporary ^3He gas depletion leads to development of new alternative detection elements. Although the other neutron gas detector, BF_3 gas proportional counter has been sometimes investigated, it did not sufficiently fulfill the requirements for neutron detectors, such as neutron detection efficiency, gas gain, and gamma sensitivity which are inferior to those of the ^3He gas detectors (Rezaei-Ochbelagh, 2012).

Inorganic neutron scintillators can be one of the solutions to replace the ^3He gas detectors. A single crystal of Eu:LiI, a mixture of ^6LiF and Ag:ZnS powders, and ^6Li loaded glass scintillator are well known traditional neutron scintillators (Eijk, 2004). Although these

* Corresponding author. Tokuyama Corporation, Shibuya 3-chome, Shibuya-ku, Tokyo 150-8383, Japan. Tel.: +81 90 5373 1732.
E-mail addresses: n-kawaguchi@tokuyama.co.jp, kawaguchi@imr.tohoku.ac.jp (N. Kawaguchi).

1350-4487/$ – see front matter © 2013 Elsevier Ltd. All rights reserved.
http://dx.doi.org/10.1016/j.radmeas.2013.03.024

scintillators show good neutron response based on $^{6}Li(n,\alpha)^{3}H$ reaction with high Q-value of 4.8 MeV, they are not fully valuable replacement for the ^{3}He detectors. Eu:LiI single crystal is significantly hygroscopic and needs to be packaged. The mixture of ^{6}LiF and Ag:ZnS powders is an opaque thin film and shows a low neutron detection efficiency. In contrast, colquiriite-type fluorides crystals such as $LiCaAlF_6$ (LiCAF) and $LiSrAlF_6$ (LiSAF) are known as host crystals of novel neutron scintillators which have are highly transparent and non-hygroscopic. Ce doped LiCAF (Yoshikawa et al., 2009, Yanagida et al., 2009a), Eu doped LiCAF (Yanagida et al., 2011a; Kawaguchi et al., 2008), Ce doped LiSAF, and Eu doped LiSAF (Yanagida et al., 2011b) showed suitable or superior scintillation properties. Higher light yield is first observed at Ce, Na codoped LiCAF (Yokota et al., 2011). Similar tendency is observed at the Eu and Na co-coped LiCAF. The light yield of Eu and Na codoped LiCAF (Yanagida et al., 2011c) is 4–5 times higher than that of conventional ^{6}Li-loaded glass scintillator. In addition, LiCAF-based neutron scintillators have low gamma-ray background due to lower effective atomic number ($Z_{eff} = 14$) and lower density of 2.98 g/cm^3 when compared to ^{6}Li loaded glass and LiSAF scintillators. Scintillation properties of the other rare-earth ions doped LiCAF have been shown. Tm or Er doped LiCAF (Yoshikawa et al., 2010), Pr doped LiCAF (Yanagida et al., 2009b), and Nd doped LiCAF (Yanagida et al., 2012) were found to have light yield lower than Eu or Ce-doped LiCAF. However in LiCAF crystals, there is still a room for improvement and trying new doping ions. Neutron responses of LiCAF doped by 3d-transition metal ions (Ti, V, Cr, Mn, Fe, Co, Ni and Cu) have not been reported yet.

In the present work, we investigated the thermal neutron detection efficiency of LiCAF scintillation crystals doped with 3d-transition metal ions. The optical and scintillation properties of Ti, V, Mn, Fe, Co, Ni and Cu doped LiCAF crystals were evaluated. Finally, thermal neutron response of Mn:LiCAF coupled with a Si avalanche photodiode (Si-APD) was investigated using T2-3 thermal neutron beam port (MUSASI port) at Japan Research Reactor-3 (JRR-3).

2. Experimental

2.1. Crystal growth

Ti, V, Mn, Fe, Co, Ni and Cu doped LiCAF were grown by the micro-pulling-down (μ-PD) method (Yoshikawa et al., 2004; Yoshikawa et al., 2007). The chamber was equipped with CaF_2 window for visual observation of the solid/liquid interface to control the growth temperature using a charge coupled device (CCD) camera as a monitor. A high-purity graphite crucible was used and inductively heated using a radio-frequency generator. Starting materials were prepared from the stoichiometric mixture of TiF_3, VF_3, MnF_2, FeF_2, CoF_2, NiF_2, CuF_2, LiF, CaF_2 and AlF_3 powders. They were thoroughly mixed and put into graphite crucibles. First, the chamber was evacuated up to 10^{-4} Torr. Then, the crucible was heated up to 400 °C and was kept for about 1 h at this temperature to remove oxygen traces caused by moisture of raw materials and adsorbates on the chamber surface. During this baking procedure, the chamber was further evacuated down to 10^{-5} Torr. After the baking, the recipient was filled with high purity Ar gas (99.999%) and CF_4 gas (99.999%) until the ambient pressure. Finally, the crucible was heated up to the melting temperature of LiCAF (~820 °C). The growth rate was 0.1 mm/min.

2.2. Optical and radioluminescence measurements

Grown crystals were cut and polished to a size of $2 \times 10 \times 1^{t}$ mm^3. Transmittance of the sample pieces were measured by JASCO V530 spectrometer, and α-ray induced emission spectra by ^{241}Am 5.5 MeV α-ray source (4 MBq) with Edinburgh Instruments FLS920 with 1 nm resolution. The detailed explanation about the α-ray radioluminescence spectrum is given in the reference (Yanagida et al., 2011d). Transmittance and emission spectra were measured from the wide surface of the sample.

2.3. Thermal neutron detection with Si-APD

In order to evaluate thermal neutron induced scintillation response, Mn doped LiCAF scintillator was coupled with a Si-APD (Hamamatsu S8664-1010) using an optical grease (OKEN 6262A). Mn:LiCAF scintillator exhibited the highest radio-luminescence intensity among present samples. The basic parameters of the used Si-APD (not the same one but the same series) can be found in Yanagida et al. (2011e). The MUSASI port in JRR-3 was used as the thermal neutron beam source. This beam source generates thermal neutrons with a flux of 800,000 n/cm^2/s at the beam port (5 cm × 5 cm). The neutron energy was fixed as 13.5 meV using the Pyloric Graphite crystal monochromator. The Si-APD was connected with a picoampermeter (KEITHLEY 237 HIGH VOLTAGE SOURCE MEASURE UNIT) which acted as high voltage supply and a current meter. The output current was recorded in a voltage range of 300–400 V with every 1 V under thermal neutron irradiation. A removable 1 mm thick Cd metal board was put between the sample and the beam port as a passive shield to compare the signal output and the background. Because the neutron energy was 13.5 meV, these thermal neutrons were fully absorbed by 1 mm thick Cd.

3. Results and discussions

3.1. Crystal elaboration

3d-transition metal ions doped LiCAF crystals were successfully grown by the μ-PD method. Grown crystals were cut and polished to a physical size of approximately $2 \times 10 \times 1^{t}$ mm^3. Appearance of cut and polished Mn doped LiCAF is shown in the inset of Fig. 1. The crystal had no cracks and looked visibly transparent.

3.2. Optical and radioluminescence properties

Radioluminescence spectra of 3d-transition metal ions doped LiCAF crystals were evaluated under ^{241}Am 5.5 MeV α-ray excitation. Unfortunately, no emission peaks were detected in Ti, V, Fe

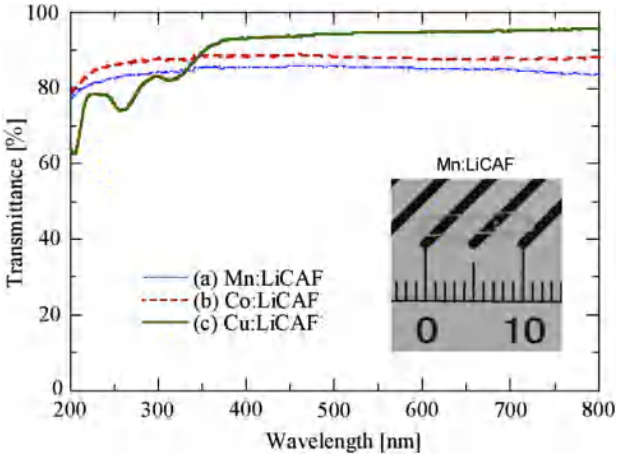

Fig. 1. Transmittance spectra of Mn, Co, and Cu, doped LiCAF with photograph of Mn doped LiCAF single crystal.

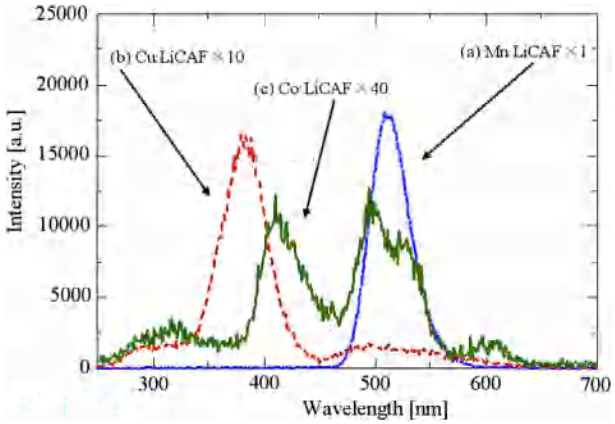

Fig. 2. ^{241}Am α-ray excited radioluminescence spectrum of Mn, Co, and Cu, doped LiCAF.

and Ni doped LiCAF around the wavelength of 200–800 nm which was a sensitivity range of standard photodetectors such as a photomultiplier and a Si photodiode. On the other hand, Mn, Co and Cu doped LiCAF showed clear emission peaks.

Mn doped LiCAF has the highest emission intensity among these crystals and the emission bands peaked at wavelength of 520 nm, as shown in Fig. 2(a). The luminescence band was assigned to $^4T_{1g} \rightarrow {}^6A_{1g}$ transition of Mn^{2+} ions in LiCAF host. Then, Fig. 1 displays the transmission spectrum of three LiCAF samples. In Mn:LiCAF, no absorption bands were observed and it was consistent with the previous results reported in True et al. (2004), where the excitation bands only in the VUV region were found.

Radioluminescence spectrum of Co-doped LiCAF is shown in Fig. 2 (curve b). Broad emission peaks were observed around wavelengths of 320, 410, 505, 530 and 600 nm. Luminescence properties of Co-doped LiCAF was not previously researched, however, these peaks were similar to those of Co doped CaF_2 and Co doped SrF_2 (Alcalá and Alonso, 1979, 1981). Differences between Co-doped LiCAF and Co-doped CaF_2 or SrF_2 at wavelength around 300–450 nm could be explained by the overlap with the emission bands of self-trapped exciton (STE) of CaF_2 and SrF_2. In the transmittance spectrum in Fig. 1(curve b) no clear absorption bands were observed.

Radioluminescence spectrum and transmittance spectrum of Cu doped LiCAF are displayed in Fig. 2 (curve c) and Fig. 1 (curve c), respectively. Emission and absorption bands can be ascribed to $^1A_{1g} \rightarrow {}^1E_g$ and $^1A_{1g} \rightarrow {}^1T_{2g}$ transitions, according to previously reported results on Cu-doped LiF (Nepomnyashchikh et al., 2011). Among present samples with detectable scintillation light, the emission intensity of Cu-doped LiCAF was weaker than that of the Mn doped one.

3.3. Thermal neutron detection with Si-APD

Among LiCAF crystals doped with 3d-transition ions, the Mn doped one showed the highest emission intensity. Therefore we tried to detect thermal neutrons with Mn doped LiCAF coupled with the Si-APD in the current (integrated) mode because luminescence of Mn ions was known to show slow luminescence with ms-scale decay time and was difficult to be detected in the photon counting (pulse height) mode. Fig. 3 shows I–V curves characterizing the used Si-APD detection system. When the Si-APD was irradiated with neutrons, slightly small change was observed when the Cd shield was introduced or removed. It could be caused possibly due to background gamma-rays from environment or from Cd shield which could emit gamma-rays upon neutron absorption.

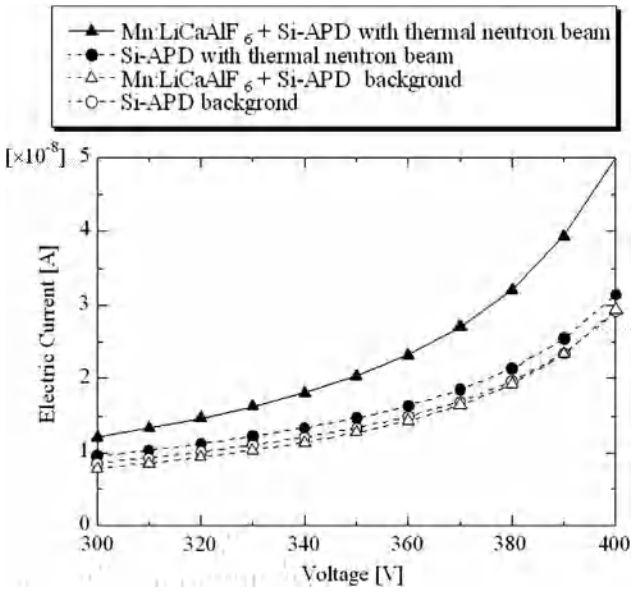

Fig. 3. I–V curves of Si-APD with no sample and Mn doped LiCAF under thermal neutron irradiation (without Cd plate) or no irradiation (with Cd plate).

As it is a common characteristic for the Si-APD, the output current increased with the increasing bias voltage due to the internal avalanche gain. Although detailed device structure and doping impurities of this Si-APD are not published, if B or Li is introduced, the APD itself could be slightly sensitive to thermal neutrons. Fig. 3 also represents the I–V profile of the Si-APD coupled with Mn doped LiCAF with and without the Cd shield. It was clear that the background levels of the Si-APD itself and the Si-APD coupled with Mn doped LiCAF were almost the same. When Mn doped LiCAF was irradiated by thermal neutrons without the Cd shield, the output current clearly exceeded the background level. This is a clear evidence that Mn doped LiCAF can detect thermal neutrons and converts neutrons to scintillation photons. Thus, Mn doped LiCAF successfully worked as a neutron scintillator in the current mode.

4. Conclusions

Ti, V, Mn, Fe, Co, Ni and Cu doped LiCAF crystals were grown by the μ-PD method. Among them, Mn, Co and Cu doped LiCAF crystals exhibited clear emission peaks under ^{241}Am α-ray excitation simulating ^{6}Li(n, α)^{3}H reaction, and Mn:LiCAF showed the highest emission intensity. Finally, Mn:LiCAF coupled with the Si-APD was irradiated by 13.5 meV thermal neutron flux in JRR-3 and as a result, Mn doped LiCAF exhibited a clear neutron signal.

Acknowledgments

The MUSASI beam port in JRR-3 was used as the thermal neutron beam source. A part of this work was conducted under the trial-use program for neutron industrial applications funded by the Ministry of Education, Culture, Sports, Science and Technology in Japan. This work is also partially supported by the funding program for next generation world-leading researchers, Japan Society for Promotion of Science.

References

Alcalá, R., Alonso, P.J., 1979. Luminescence in x-irradiated CaF_2:Co. J. Lumin. 20, 1–8.
Alcalá, R., González, C., Alonso, P.J., 1981. Charge change processes of 3d-ions in doped SrF_2. J. Lumin. 26, 141–151.

Eijk, C.W.E., 2004. Inorganic scintillators for thermal neutron detection. Radiat. Meas. 38, 337–342.

Kawaguchi, N., Yanagida, T., Novoselov, A., Kim, K.J., Fukuda, K., Yoshikawa, A., Miyake, M., Baba, M., 2008. Neutron responses of Eu^{2+} activated $LiCaAlF_6$ scintillator. In: NSS/MIC. 2008 IEEE, pp. 1174–1176.

Nepomnyashchikh, A.I., Shalaev, A.A., Subanakov, A.K., Paklin, A.S., Bobina, N.S., Myasnikova, A.S., Shendrik, R. Yu, 2011. Impurity Cu^{+} centers in LiF single crystals. Opt. Spectrosc. 111, 411–414.

Nikitin, A., Bliven, S., 2010. Needs of well logging industry in new nuclear detectors. In: NSS/MIC. 2010 IEEE, pp. 1214–1219.

Rezaei-Ochbelagh, D., 2012. Comparison of ^3He and BF_3 neutron detectors used to detect hydrogenous material buried in soil. Radiat. Phys. Chem. 81, 379–382.

True, M., Kirm, M., Negodine, E., Vielhauer, S., Zimmerer, G., 2004. VUV spectroscopy of Tm^{3+} and Mn^{2+} doped $LiSrAlF_6$. J. Alloys Compd. 374, 36–39.

Yamaoka, K., Ohno, M., Terada, Y., Hong, S., Kotoku, J., Okada, Y., Tsutsui, A., Endo, Y., Abe, K., Fukazawa, Y., Hirakuri, S., Hiruta, T., Itoh, K., Kamae, T., Kawaharada, M., Kawano, N., Kawashima, K., Kishishita, T., Kitaguchi, T., Kokubun, M., Madejski, G.M., Makishima, K., Mitani, T., Miyawaki, R., Murakami, T., Murashima, M.M., Nakazawa, K., Niko, H., Nomachi, M., Oonuki, K., Sato, G., Suzuki, M., Takahashi, H., Takahashi, I., Takahashi, T., Takeda, S., Tamura, T., Tanaka, T., Tashiro, M., Watanabe, S., Yanagida, T., Yonetoku, 2005. Development of the HXD-II wideband all-sky monitor onboard Astro-E2. IEEE Trans. Nucl. Sci. 52, 2765–2772.

Yanagida, T., Yoshikawa, A., Yokota, Y., Maeo, S., Kawaguchi, N., Ishizu, S., Fukuda, K., Suyama, T., 2009a. Crystal growth, optical properties, and alpha-ray responses of Ce doped $LiCaAlF_6$ for different Ce concentration. Opt. Mater. 32, 311–314.

Yanagida, T., Yoshikawa, A., Yokota, Y., Fujimoto, Y., Kawaguchi, N., Ishizu, S., Fukuda, K., Suyama, T., 2009b. Crystal growth and luminescence properties of Pr doped $LiYF_4$ and $LiCaAlF_6$. Jpn. J. Appl. Phys. 48, 085503.

Yanagida, T., Yoshikawa, A., Yokota, Y., Kamada, K., Usuki, Y., Yamamoto, S., Miyake, M., Baba, M., Sasaki, K., Ito, M., 2010. Development of Pr:LuAG scintillator array and assembly for positron emission mammography. IEEE Nucl. Trans. Sci. 57, 1492–1495.

Yanagida, T., Kawaguchi, N., Fujimoto, Y., Fukuda, K., Yokota, Y., Yamazaki, A., Watanabe, K., Pejchal, J., Uritani, A., Iguchi, T., Yoshikawa, A., 2011a. Basic study of Europium doped $LiCaAlF_6$ scintillator and its capability for thermal neutron imaging application. Opt. Mater. 33, 1243–1247.

Yanagida, T., Kawaguchi, N., Fujimoto, Y., Yokota, Y., Yamazaki, A., Watanabe, K., Kamada, K., Yoshikawa, A., Chani, V., 2011b. Ce and Eu doped $LiSrAlF_6$ scintillators for neutron detectors. Radiat. Meas. 46, 1708–1711.

Yanagida, T., Yamaji, A., Kawaguchi, N., Fujimoto, Y., Fukuda, K., Kurosawa, S., Yamazaki, A., Watanabe, K., Futami, Y., Yokota, Y., Uritani, A., Iguchi, T., Yoshikawa, A., Nikl, M., 2011c. Europium and sodium codoped $LiCaAlF_6$ scintillator for neutron detection. Appl. Phys. Express 4, 106401.

Yanagida, T., Kamada, K., Fujimoto, Y., Yokota, Y., Yoshikawa, A., Yagi, H., Yanagitani, T., 2011d. Scintillation properties of transparent ceramic and single crystalline Nd:YAG scintillators. Nucl. Instr. Meth. A 631, 54–57.

Yanagida, T., Fukabori, A., Fujimoto, Y., Ikesue, A., Kamada, K., Kataoka, J., Yokota, Y., Yoshikawa, A., Chani, V., 2011e. Scintillation properties of transparent $Lu_3Al_5O_{12}$ (LuAG) ceramics doped with different concentrations of Pr^{3+}. Phys. Status. Solidi (c) 8, 140–143.

Yanagida, T., Futami, Y., Kawaguchi, N., Pejchal, J., Fujimoto, Y., Kurosawa, S., Yokota, Y., Yoshikawa, A., 2012. Nd^{3+} doped $LiCaAlF_6$ single crystal for scintillator application. Key Eng. Mater. 508, 224–229.

Yokota, Y., Fujimoto, Y., Yanagida, T., Takahashi, H., Yonetani, M., Hayashi, K., Park, I., Kawaguchi, N., 2011. Crystal growth of Na-co-doped Ce:$LiCaAlF_6$ single crystals and their optical, scintillation, and physical properties. Crystal Growth Des. 11, 4775–4779.

Yoshikawa, A., Satonaga, T., Kamada, K., Sato, H., Nikl, M., Solovieva, N., Fukuda, T., 2004. J. Cryst. Growth 270, 427–432.

Yoshikawa, A., Nikl, M., Boulon, G., Fukuda, T., 2007. Opt. Mater. 30, 6–10.

Yoshikawa, A., Yanagid, T., Yokota, Y., Kawaguchi, N., Ishizu, S., Fukuda, K., Suyama, T., Kim, K.J., Nikl, M., Miyake, M., Baba, M., 2009. Single crystal growth, optical properties and neutron responses of Ce^{3+} doped $LiCaAlF_6$. IEEE Trans. Nucl. Sci. 56, 3796–3799.

Yoshikawa, A., Yanagida, T., Yokota, Y., Nara, F., Fujimoto, Y., Pejchal, J., Kawaguchi, N., Ishizu, S., Fukuda, K., Suyama, T., Nikl, M., 2010. Crystal growth and VUV luminescence properties of Er doped and Tm doped $LiCaAlF_6$. Opt. Mater. 32, 845–849.